Synthesis of fibre reinforced Al$_2$O$_3$−SiO$_2$ aerogel composite with high density uniformity via a facile high-pressure impregnation approach

Gang Yang, Yonggang Jiang*, Junzong Feng, Sizhao Zhang, Jian Feng

Science and Technology on Advanced Ceramic Fibers and Composites Laboratory, National University of Defense Technology, Changsha Hunan 410073, PR China

Abstract

Alumina-silica (Al$_2$O$_3$−SiO$_2$) aerogel composite, with low density, low thermal conductivity and high-temperature stability, is attracting increased interest in the field of thermal insulation application. In this paper, a novel way to fabricate fibre reinforced Al$_2$O$_3$−SiO$_2$ aerogel composite via a facile high-pressure impregnation approach was reported. Two Al$_2$O$_3$−SiO$_2$ aerogel composites, HPe and LPe, were synthesized via high-pressure and low-pressure impregnation approach, respectively. The effects of the impregnation approach on the aerogel composites performance were studied, and the impregnation model was established. The results showed that the as-prepared HPe exhibited higher density uniformity, better high-temperature stability, higher specific surface area and lower thermal conductivity. It was also shown that the effect of impregnation approach on the mean density and morphology of the aerogel composites is negligible. However, the standard deviation of density (0.00857) and mean thickness shrinkage (9.98%) of HPe were 37.8% and 15.4% lower than that of LPe, respectively. The specific surface area (884.1 m^2/g) of HPe was 43.5% higher than that of LPe. The thermal conductivity of HPe at 1100 °C was 2.74% lower than that of LPe. The impregnation model of the aerogel composites presented that the density uniformity and thermal conductivity of HPe were improved obviously, because there were less large pores in HPe than in the LPe.

Keywords: Al$_2$O$_3$−SiO$_2$ aerogel composites, density uniformity, thermal insulation, pressure impregnation

I. Introduction

Fibre reinforced silica aerogel composite, with low thermal conductivity and high mechanical performance, expands its uses especially as an excellent thermal insulation material [1–11]. However, alumina-silica (Al$_2$O$_3$−SiO$_2$) aerogel, with high specific surface area, high porosity and high temperature stability [12–17], is attracting more increased interest in the field of thermal insulation application [18–25] at elevated temperature. As with SiO$_2$ aerogel, the Al$_2$O$_3$−SiO$_2$ aerogel is fragile and difficult to use directly. Recently, mullite fibres reinforced Al$_2$O$_3$−SiO$_2$ aerogel composites (M$_f$/ASAC) [26–28] were synthesized, which exhibited high mechanical properties and low thermal conductivity.

Our research results, however, showed that the density uniformity of the M$_f$/ASAC needs to be improved.

The question we meet is how to decrease the large pores and to improve the density uniformity of the M$_f$/ASAC. Lots of studies demonstrated the large impact of high-pressure impregnation technique on the composite properties [29,30]. For example, Locs *et al.* [29] moved wood and SiO$_2$ sol to a hydraulic isostatic press with the pressure increase up to 30, 60 and 125 MPa in the process of fabricating SiC ceramics. The results showed that high-pressure impregnation approach was highly effective for the introduction of SiO$_2$ sol into the wood, relative impregnation efficiency increases from 45% up to 95%, and the uniformity of density was improved.

The objective of this study is to establish an understanding of the influence of impregnation approach on the M$_f$/ASAC. In the present work, the M$_f$/ASAC with high density uniformity is fabricated via a novel facile high-pressure impregnation approach. The influence of impregnation approach on the aerogel composites and impregnation model are studied. The density uniformity, high-temperature stability, specific surface area

*Corresponding author: tel: +86 731 84573169,
fax: +86 731 84576578, e-mail: *jygemail@163.com*

and thermal conductivity are improved significantly by the high-pressure impregnation approach.

II. Experimental

Al_2O_3–SiO_2 sol was synthesized via sol-gel method [27] by using aluminium tri-sec-butoxide (ASB) and tetraethoxysilane (TEOS) as precursors (purchased from Sinopharm Chemical Reagent Co., Ltd), and the ethanol (EtOH) as solvent. Ethyl acetoacetate (Etac) was added to control the speed of hydrolysis. The typical mole ratio was ASB : TEOS : EtOH : H_2O : Etac = 3 : 1 : 52 : 4.6 : 0.39. Mullite fibre mat was a type of high temperature insulation blanket, which was composed of inorganic mullite fibres and used as reinforcement of Al_2O_3–SiO_2 aerogel composites. Volume content (f_c) of mullite fibres was 7%.

Mullite fibre mat was preformed in a metal mould, and the mould with the fibre mat was then put in a sealed container. The Al_2O_3–SiO_2 sols were soaked into the mat by vacuum infiltration approach. The Al_2O_3–SiO_2 sols in the fibre mat gelled and aged in the container which kept impregnation at the pressure of 5 MPa and 0.1 MPa for 48 h, respectively. The retrieved Al_2O_3–SiO_2 wet gels reinforced by mullite fibres were dried under supercritical EtOH (10 MPa, 270 °C) to produce M_f/ASAC. The obtained M_f/ASAC samples were denoted as HPe (prepared using high-pressure impregnation at 5 MPa) and LPe (prepared using low-pressure impregnation at 0.1 MPa).

The bulk density was obtained by measuring the volume and weight of the composites. In order to assess high-temperature stability, the M_f/ASAC, samples (with dimensions of 40 × 40 × 20 mm) were calcined at 1200 °C in muffle furnace (KBF1700, China) for 1500 s. The thickness shrinkage (H) of the samples was obtained according to the following formulas:

$$H = \left(1 - \frac{H_1}{H_0}\right) \cdot 100 \tag{1}$$

where H_1 and H_0 were the thickness dimensions of the sample before and after calcination.

The thermal conductivity of the M_f/ASAC samples (with dimensions of $\varnothing 180$ mm × 20 mm) were performed by Hotplate Thermal Conductivity Analyser (PBD-12-4, China). The hot surface temperatures were set as 400, 600, 800, 1000 and 1100 °C. Specific surface area of the Al_2O_3–SiO_2 aerogel was measured by using Quantasorb surface area analyser (Autosorb-iQ2-MP, USA) with N_2 as an adsorbing gas. Pore size distribution of the Al_2O_3–SiO_2 aerogel was derived from the adsorption isotherm by using Barrett-Joyner-Halenda (BJH) theory. The morphological properties of the Al_2O_3–SiO_2 aerogel were investigated by a scanning electron microscopy (FEI Nova NanoSEM 230, USA).

III. Results and discussion

3.1. Density uniformity

Two M_f/ASAC composites (HPe and LPe) with sample dimensions of 190 mm × 190 mm × 20 mm were double side machined with computerized numerical control (CNC) equipment, and then equally divided into 16 pieces (Fig. 1a). Every piece dimension was $40 \times 40 \times 20$ mm. Figure 1b presents the density distribution of the M_f/ASAC.

It is found that the density uniformity of the M_f/ASAC samples is improved significantly by high-pressure impregnation approach. The mean density of HPe and LPe is 0.277 and 0.279 g/cm^3, but the standard deviation (SD) of HPe density is 0.00857, which is 37.8% lower than that of LPe (0.01378).

3.2. High-temperature stability

The thickness shrinkage of the M_f/ASAC samples is presented in Fig. 2. The results illustrate that the high-temperature stability of HPe (Fig. 2b) is better than that of LPe (Fig. 2a). The mean thickness shrinkage (MTS) of HPe is 9.98%, which is 15.4% lower than that of LPe (11.8%) after calcination at 1200 °C for 1500 s. The SD of thickness shrinkage is also improved via the high-pressure impregnation approach.
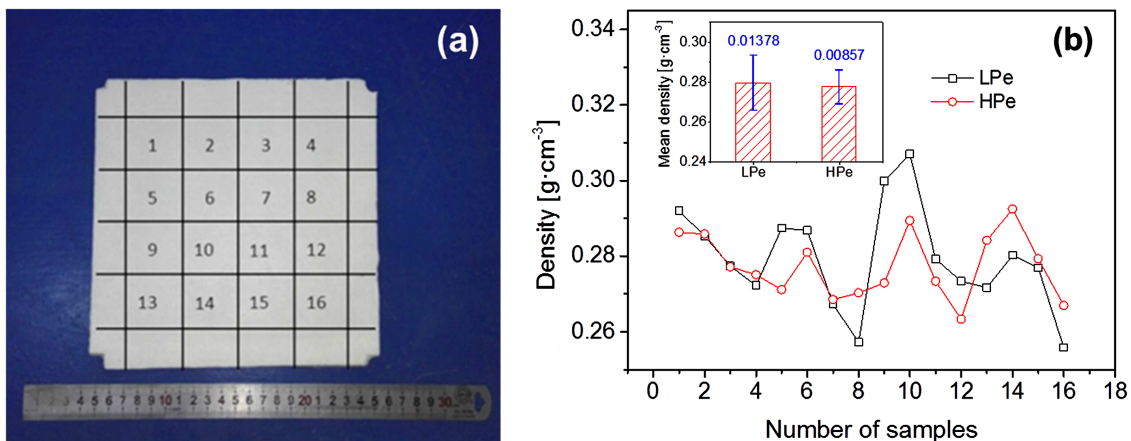

Figure 1. Al_2O_3–SiO_2 aerogel composites (a) and their density distribution (b)
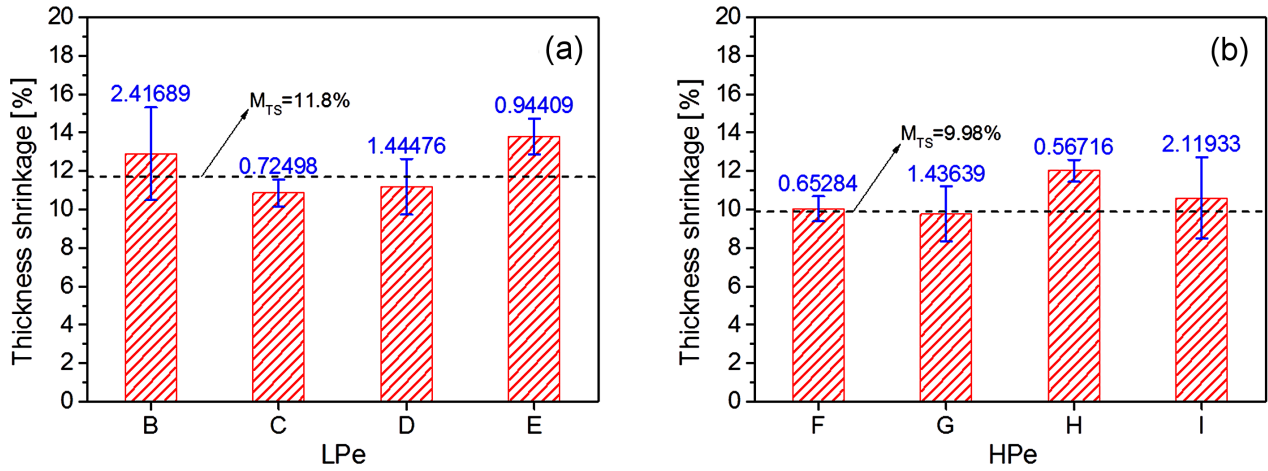
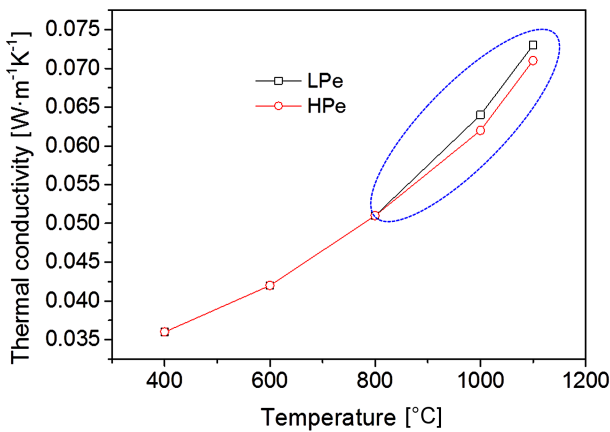**Figure 2. Thickness shrinkage of the M$_f$/ASAC samples: a) LPe and b) HPe**

Figure 3. Thermal conductivity of the M$_f$/ASAC samples

3.3. Thermal conductivity at elevated temperature

The thermal conductivity of the M$_f$/ASAC samples was recorded at elevated hot surface temperatures (400–1100 °C), as shown in Fig. 3. With the rising of temperature, the thermal conductivity of the M$_f$/ASAC samples increased slowly. The thermal conductivities of HPe and LPe were similar between the temperatures of 400 °C and 800 °C. While the thermal conductivity (0.071 W/m·K, 1100 °C) of HPe was 2.74% lower than that of LPe, and 27.5% lower than the data found in literature [28], which indicated better thermal insulation performance at elevated temperature.

3.4. Microstructures

Figure 4 shows the nitrogen adsorption isotherms and pore size distribution of Al$_2$O$_3$−SiO$_2$ aerogels. According to IUPAC classification [31], the adsorption-isotherm of the as-prepared Al$_2$O$_3$−SiO$_2$ aerogels (HPe and LPe) is Type V isotherm, and the adsorption hysteresis is Type H3 loop, which exhibits adsorption at high P/P_0 and aggregates of plate-like particles giving rise to slit-shaped pores.

Figure 4b indicates that the average pore diameter of HPe and LPe are 47.6 nm and 47.9 nm, respectively. The average pore diameter is smaller than that of air mean free path (66 nm, 1 atm, 23 °C) [32], which is advantageous to reduce the thermal conductivity of the Al$_2$O$_3$−SiO$_2$ aerogel composites. The specific surface area of HPe (884.1 m^2/g) is 43.5% higher than that of LPe (616.3 m^2/g) and 17.9% higher than the reported value (750 m^2/g) [24].
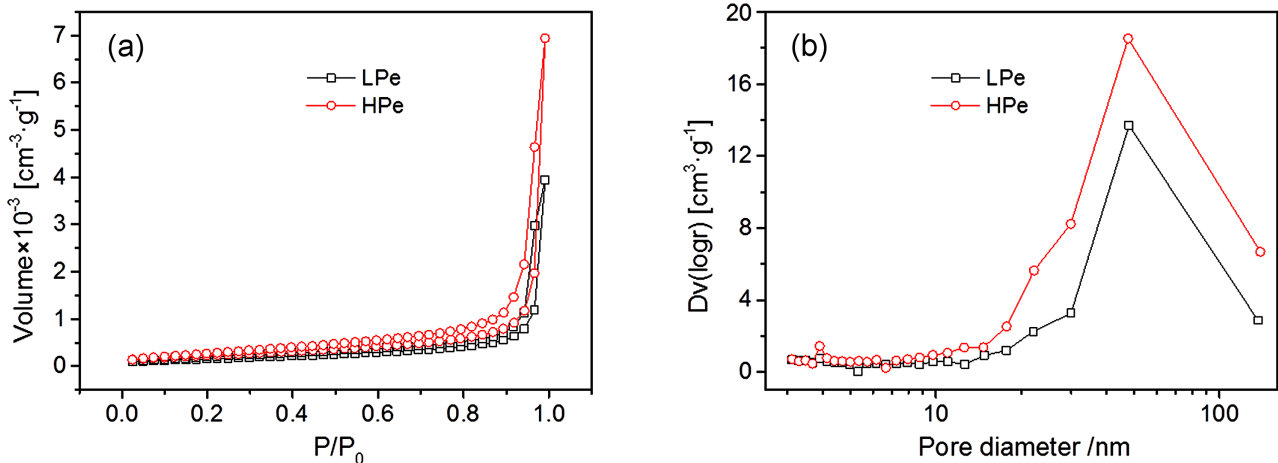

Figure 4. Nitrogen adsorption isotherms (a) and pore size distribution (b) of HPe and LPe samples
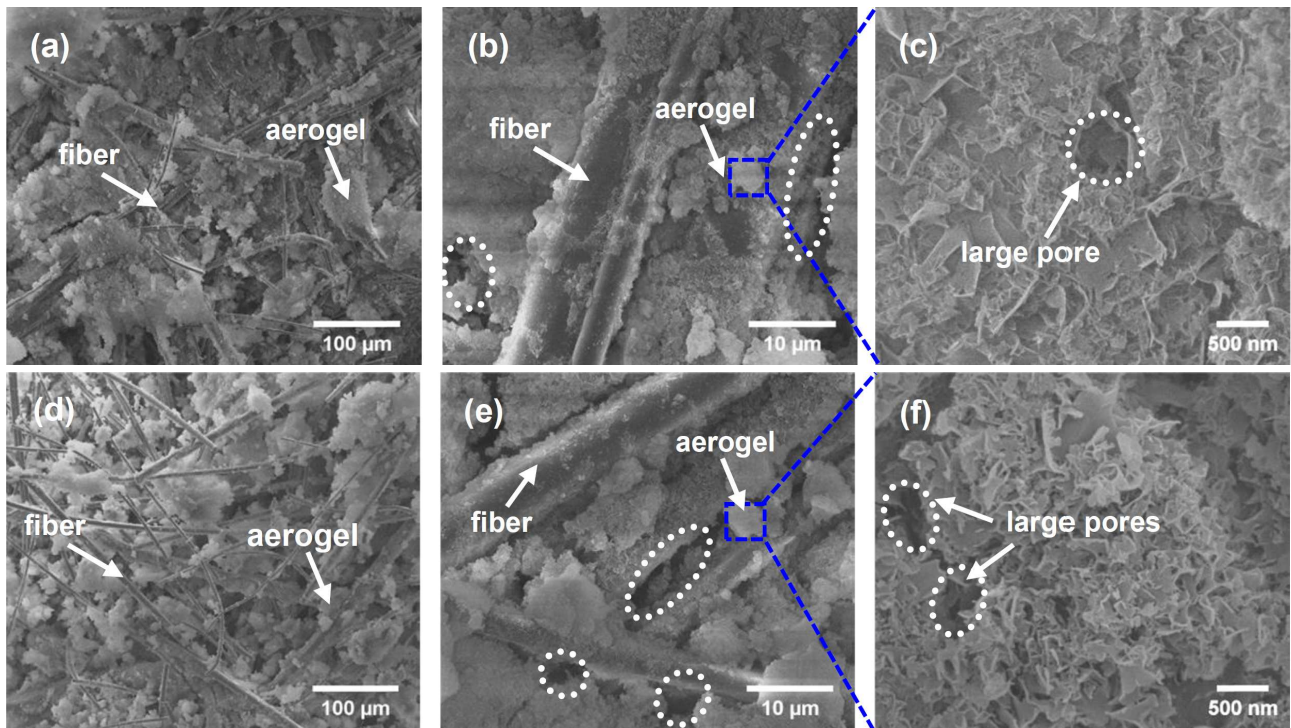
Figure 5. SEM images of HPe (a, b, c) and LPe (d, e, f) samples

SEM images of HPe and LPe are presented in Fig. 5. As it can be seen, the morphology of HPe and LPe is similar. The mullite fibres are surrounded by plate-like $Al_2O_3-SiO_2$ aerogels (Figs. 5c and 5f), and lots of small slit-shaped pores and large pores can be found. Figures 5b,e show that LPe contains larger pores than HPe. This indicates that high-impregnation pressure is propitious to decrease the large pores. It is consistent with the above results of HPe with the higher specific surface area and lower thermal conductivity.

3.5. Impregnation model of aerogel composites

The schematic impregnation model of HPe and LPe is presented in Fig. 6. The mullite fibre mat is consisted of mullite fibres disorderly arranged in the in-plane direction, and lots of large pores can be found in the mat. When it is soaked in the $Al_2O_3-SiO_2$ sol via vacuum infiltration approach, the mat is filled with sol. The $Al_2O_3-SiO_2$ sols gelled and aged in the container which kept the pressure at 5 MPa and 0.1 MPa for 48 h. During the soaking process, lots of small air bubbles in the sol remained in the mullite fibre mat. With high-pressure impregnation approach, the air bubbles were compressed and their diameter decreased. The bubbles were fixed in subsequent gelation and supercritical drying process. Consequently, there were smaller amount of large pores in HPe than in LPe (Fig. 5b), which was propitious to decrease the thermal conductivity of HPe at elevated temperature (Fig. 3). In general, the M_f/ASAC samples with higher density unifor-
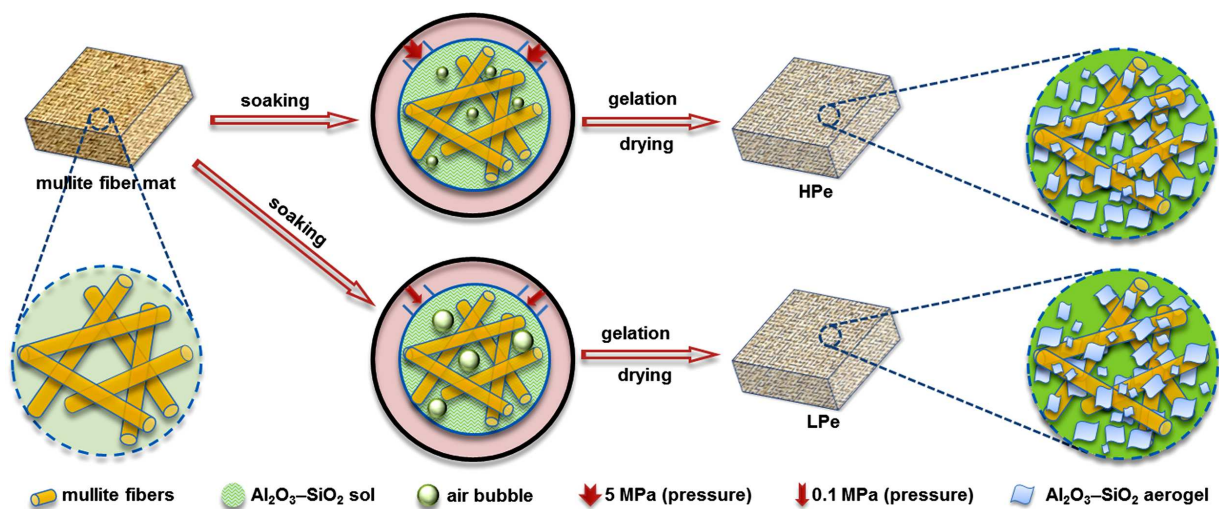

Figure 6. Schematic impregnation model of HPe and LPe

mity (Fig. 1), better high-temperature stability (Fig. 2), higher specific surface area and lower thermal conductivity (Fig. 3) can be synthesized via the facile high-pressure impregnation approach.

IV. Conclusions

Mullite fibre reinforced $Al_2O_3-SiO_2$ aerogel composites, HPe and LPe, were fabricated via a novel facile high-pressure and low-pressure impregnation approach, respectively. The effects of impregnation approach on the aerogel composites performance were studied, and the impregnation model was established.

No impregnation approach effects on the mean density and morphology of the $Al_2O_3-SiO_2$ aerogel composites were observed. The mean density of HPe and LPe is 0.277 and 0.279 g/cm^3, respectively, and morphologies of HPe and LPe are similar. Nevertheless, the standard deviation of density (0.00857) and mean thickness shrinkage (9.98%) of HPe were 37.8% and 15.4% lower than that of LPe. The specific surface area (884.1 m^2/g) of HPe was 43.5% higher than that of LPe. The thermal conductivity of HPe at 1100 °C was 2.74% lower than that of LPe. The impregnation model of the aerogel composites presented that the air bubbles in sol were compressed via high-pressure impregnation process, and were fixed in subsequent gelation and supercritical drying process. The density uniformity and thermal conductivity of HPe were improved obviously, because there were less large pores in HPe than in the LPe. The as-prepared HPe aerogel composite is an excellent thermal insulation material with higher density uniformity, better high-temperature stability, higher specific surface area and lower thermal conductivity.

References

1. G.R. Cunnington, S.C. Lee, S.M. White, "Radiation heat transfer in fiber-filled silica aerogel - Comparison of theory with experiment", AIAA 97-3884, *National Heat Transfer Conference*, Baltimore, MD, U.S.A, 1997.
2. J. Chandradass, S. Kang, D.S. Bae, "Synthesis of silica aerogel blanket by ambient drying method using water glass based precursor and glass wool modified by alumina sol", *J. Non-Cryst. Solids*, **354** (2008) 4115–4119.
3. Q. Gao, J. Feng, C. Zhang, J. Feng, W. Wu, Y. Jiang, "Mechanical properties of ceramic fiber-reinforced silica aerogel insulation composites", *J. Chinese Ceram. Soc.*, **37** (2009) 1–5.
4. M. Koebel, A. Rigacci, P. Achard, "Aerogel-based thermal superinsulation: an overview", *J. Sol-Gel Sci. Technol.*, **63** (2012) 315–339.
5. X. Li, Q. Wang, H. Li, H. Ji, X. Sun, J. He, "Effect of sepiolite fiber on the structure and properties of the sepiolite/silica aerogel composite", *J. Sol-Gel Sci. Technol.*, **67** (2013) 646–653.
6. C. Mi, Y. Jiang, D. Shi, S. Han, Y. Sun, X. Yang, J. Feng, "Mechanical property test of ceramic fiber reinforced silica aerogel composites", *Acta Mater. Compos. Sin.*, **31** (2014) 635–643.
7. A. Shaid, M. Furgusson, L. Wang, "Thermophysiological comfort analysis of aerogel nanoparticle incorporated fabric for fire fighter's protective clothing", *Chem. Mater. Eng.*, **2** (2014) 37–43.
8. Z. Shao, X. He, Z. Niu, T. Huang, X. Cheng, Y. Zhang, "Ambient pressure dried shape-controllable sodium silicate based composite silica aerogel monoliths", *Mater. Chem. Phys.*, **162** (2015) 346–353.
9. X. Shi, R. Zhang, S. He, Z. Li, W. Cao, X. Cheng, "Synthesis and heat insulation performance of glass fiber reinforced SiO_2 aerogel composites", *J. Chinese Ceram. Soc.*, **44** (2016) 129–136.
10. E.S. Park, T.S. Kwak, Y.H. Na, H.J. Song, H.S. Lee, S.H. Hong, "Composition for forming silica based insulating layer, silica based insulating layer and method for manufacturing silica based insulating layer", US patent 9 362 030 B2, June, 2016.
11. C. Li, X. Cheng, Z. Li, Y. Pan, Y. Huang, L. Gong, "Mechanical, thermal and flammability properties of glass fiber film/silica aerogel composites", *J. Non-Cryst. Solids*, **457** (2017) 52–59.
12. P.R. Aravind, P. Mukundan, P.K. Pillai, K.G. Warrier, "Mesoporous silica-alumina aerogels with high thermal pore stability through hybrid sol-gel route followed by subcritical drying", *Micropor. Mesopor. Mater.*, **96** (2006) 14–20.
13. T. Osaki, K. Nagashima, K. Watari, K. Tajir, "Silica-doped alumina cryogels with high thermal stability", *J. Non-Cryst. Solids*, **353** (2007) 2436–2442.
14. P.R. Aravind, P. Shajesh, S. Smitha, P. Mukundan, K.G. Warrier, "Nonsupercritically dried silica-alumina aerogels - Effect of gelation pH", *J. Am. Ceram. Soc.*, **91** (2008) 1326–1328.
15. F.I. Hurwitz, H. Guo, K.N. Newlin, "Influence of boehmite precursor on aluminosilicate aerogel pore structure, phase stability and resistance to densification at high temperatures", *Polym. Preprints*, **52** (2011) 16–17.
16. X. Wu, G. Shao, S. Cui, L. Wang, X. Shen, "Synthesis of a novel $Al_2O_3-SiO_2$ composite aerogel with high specific surface area at elevated temperatures using inexpensive inorganic salt of aluminum", *Ceram. Int.*, **42** (2016) 874–882.
17. X. Wu, G. Shao, X. Shen, S. Cui, L. Wang, "Novel $Al_2O_3-SiO_2$ composite aerogels with high specific surface area at elevated temperatures with different alumina/silica molar ratios prepared by a non-alkoxide sol-gel method", *RSC Adv.*, **6** (2016) 5611–5620.
18. F.I. Hurwitz, G.C. Mbah, "High temperature aerogels for thermal protection systems", *32nd Annual Conference on Composite Materials and Structures*, Daytona Beach, FL, January, 2008.
19. W. Wu, J. Feng, C. Zhang, Q. Gao, J. Feng, Y. Jiang, "Preparation and properties of $Al_2O_3-SiO_2$ aerogels", *Mater. Rev.*, **22** (2008) 349–352.
20. J. Feng, Q. Gao, W. Wu, C. Zhang, J. Feng, Y. Jiang, "Effect of silica content on structure and properties of $Al_2O_3-SiO_2$ aerogels", *Chinese J. Inorg. Chem.*, **25** (2009) 1758–1763.
21. R. Trifu, W. Rhine, I. Melnikova, S. White, F. Hurwitz, "Aluminum silicate aerogels with high temperature stability",, in *Advances in Bioceramics and Porous Ceramics II*

(Eds. R. Narayan, P. Colombo, D. Singh and J. Salem), John Wiley & Sons, Inc., Hoboken 2009.

22. F.I. Hurwitz, M. Gallagher, T.C. Olin, M.K. Shave, M.A. Ittes, K.N. Olafson, M.G. Fields, R.B. Rogers, "Optimization of alumina and aluminosilicate aerogel structure for high-temperature performance", *Int. J. Appl. Glass Sci.*, **5** (2014) 276–286.

23. T. Fu, J. Tang, K. Chen, F. Zhang, "Scattering and absorption coefficients of silica-doped alumina aerogels", *Appl. Optics*, **55** (2016) 705–711.

24. J. Yang, Q. Wang, T. Wang, Y. Liang, "Facile one-step precursor-to-aerogel synthesis of silica-doped alumina aerogels with high specific surface area at elevated temperatures", *J. Porous. Mater.*, **24** (2017) 889–897.

25. W. Wang, Z. Zhang, G. Zu, J. Shen, B. Zhou, "Preparation of heat-resistant silica-alumina composite aerogel by adding trimethylethoxysilane", *Chinese J. Inorg. Chem.*, **32** (2016) 1–7.

26. X. Yang, J. Wei, D. Shi, Y. Sun, S. Lv, J. Feng, Y. Jiang, "Comparative investigation of creep behavior of ceramic fiber-reinforced alumina and silica aerogel", *Mater. Sci. Eng. A*, **609** (2014)125–130.

27. L. Xu, Y. Jiang, J. Feng, J. Feng, C. Yue, "Infrared-opacified $Al_2O_3-SiO_2$ aerogel composites reinforced by SiC-coated mullite fibers for thermal insulations", *Ceram. Int.*, **41** (2015) 437–442.

28. H. Chen, X. Sui, C. Zhou, C. Wang, C. Yin, F. Liu, "Preparation and characterization of mullite fiber-reinforced $Al_2O_3-SiO_2$ aerogel composites", *Key Eng. Mater.*, **697** (2016) 360–363.

29. J. Locs, L. Berzina-Cimdina, A. Zhurinsh, D. Loca, "Optimized vacuum/pressure sol impregnation processing of wood for the synthesis of porous, biomorphic SiC ceramics", *J. Eur. Ceram. Soc.*, **29** [8] (2009) 1513–1519.

30. S. Farhan, R. Wang, K. Li, "Directional thermophysical, ablative and compressive behavior of 3D carbon/carbon composites", *Ceram. Int.*, **41** (2015) 9763–9769.

31. K.S.W. Sing, D.H. Everett, R.A.W. Haul, L. Moscou, R.A. Pierotti, J. Rouquerol, T. Siemieniewska, "Reporting physisorption data for gas solid systems with special reference to the determination of surface area and porosity", *Pure Appl. Chem.*, **57** (1985) 603–619.

32. S.G. Jennings, "The mean free path in air", *J. Aerosol Sci.*, **19** (1988) 159–166.